Sādhanā, Vol. 17, Parts 3 & 4, September 1992, pp. 451–457. © Printed in India.

Second-order quasi-phase matched second harmonic generation in annealed proton-exchanged $LiNbO_3$ channel waveguides

R V RAMASWAMY and XIAOFAN CAO

Photonics Research Laboratory, Department of Electrical Engineering, University of Florida, Gainesville, FL 32611, USA

Abstract. We report the first efficient blue second harmonic generation (SHG) in a second-order quasi-phase matching (QPM) $LiNbO_3$ waveguide. We show both theoretically and experimentally that the second-order QPM grating is the optimum structure for waveguide SHG in $LiNbO_3$ waveguides. Using such a structure, we have demonstrated blue light generation with a conversion efficiency of 65%/W-cm^2, the highest reported so far in $LiNbO_3$ waveguides.

Keywords. Harmonic generation; optical waveguides; $LiNbO_3$ waveguides; quasi-phase matched waveguides.

1. Introduction

Optical waveguides by their very nature form an ideal medium for nonlinear optical interaction. Waveguide characteristics, such as diffractionless propagation in small volumes, high beam confinement, and hence, high optical power density, can be combined with optimized nonlinear optics materials to produce new opportunities in the development of frequency conversion and signal processing devices. Furthermore, phase matching in the guided wave geometries depends both on the waveguide geometries and the material dispersion. Hence, there are more degrees of freedom possible for producing phase matching with guided waves than with plane waves. In addition, nonlinear interaction can take place either in the guiding layer or in the substrate. Thus, efficient nonlinear interaction can potentially be implemented with any combination of linear and nonlinear materials (waveguide and substrate) for the desired performance.

Second harmonic generation (SHG) by quasi-phase matching (QPM) in $LiNbO_3$ waveguides has recently attracted a great deal of attention (Lim *et al* 1989; Webjorn *et al* 1989). Using periodically domain-inverted gratings on the Z^+ surface of $LiNbO_3$, QPM between the fundamental (pump) and second harmonic guided waves is possible for an arbitary pump wavelength λ^{ω}. Moreover, the use of d_{33}, the largest nonlinear coefficient, becomes possible. Normalized conversion efficiency of the order of few $200 \sim 300$%/W-cm^2 is theoretically achievable using this scheme (Laurell *et al* 1990). This would enable us to obtain a few milliwatts of blue radiation by direct doubling of diode lasers in the waveguide geometry. Applications of such visible sources include optical storage, reprographics, high-resolution displays and communications.

Since the first reports of the implementation of the QPM scheme in $LiNbO_3$ waveguides (Lim *et al* 1989; Webjorn *et al* 1989), several attempts have been made to improve the frequency conversion efficiency. The reported normalized efficiencies today vary from 1%/W-cm^2 for the first-order QPM grating (Laurell *et al* 1990) to $\sim$40%/W-cm^2 for the third-order grating (Fejer & Lim 1990). In all cases, the best conversion efficiency is still only a few percent of the theoretically predicted value, and the highest efficiency was observed by phase matching into the lowest order waveguide mode of the second harmonic radiation.

In this paper, we analyse various factors contributing to the reduction in the conversion efficiency, with particular emphasis on its dependence on the periodic domain inversion grating profile and depth. We compare the theoretical estimates for the case of three grating orders (first, second, and third order), and identify the second-order QPM to be the overall optimum structure. We report a normalized conversion efficiency of 65%/W-cm^2 into the blue by phase matching the first-order mode of the second harmonic radiation. To the best of our knowledge, this is the first experiment using a second-order grating, and also the largest published normalized efficiency thus far in $LiNbO_3$ waveguides. The results are explained on the basis of the domain inversion profile via a comparison of the predictions for the various grating orders.

2. Quasi-phase matched second harmonic generation

The quasi-phase matching (QPM) scheme (Bloembergen & Sievers 1970), which involves a periodic modulation of optical nonlinearity along the propagation direction, can provide the optimum mode field overlap and the possibility of using the largest nonlinear coefficient of the waveguide material. The QPM condition is given by

$$\Delta\beta = \beta_k - \beta_i - \beta_j = 2\pi q/\Lambda, \tag{1}$$

where Λ is the modulation period of the nonlinearity grating and q represents the order of the QPM grating. As seen in (1), by choosing the appropriate period, QPM condition can be satisfied for an arbitrary wavelength. If the amplitude (modulation depth) of the nonlinear grating is twice that of the nonlinear coefficient d (i.e., periodic domain inversion grating), the effective nonlinear coefficient $d_{eff} = 2d/q\pi$. To get a feeling of the advantages of QPM, a comparison of effective nonlinear coefficient for $LiNbO_3$ is given as follows. In first-order QPM scheme, the effective nonlinear coefficient $d_{eff} = 2d_{33}/\pi \sim 25$ pm/V, which is about 5 times larger than $d_{eff} = d_{31} \sim 5$ pm/V for the case of birefringent phase matching. Moreover, since QPM does not rely upon the magnitude of birefringence, arbitrary wavelengths can be quasi-phase matched.

The concept of QPM was developed in the early 60's, however, due to the difficulties in fabricating periodic nonlinear gratings with small periods (typically $< 10\,\mu$m), implementation of QPM schemes was limited to only semiconductor materials (GaAs). Recently, new developments in the studies of ferroelectric crystal domain structures have led to simple techniques to periodically reverse the crystal domains. In ferroelectrics crystals such as $LiNbO_3$, $LiTaO_3$, and KTP, the signs of the nonlinear coefficients are linked to the direction of the spontaneous electric polarization. Thus, a periodic modulation of optical nonlinearity can be accomplished through periodic ferroelectric domain reversal. Recently, many techniques were discovered for achieving micro-domain inversion in $LiNbO_3$. For example, domain reversal can occur as a result of titanium diffusion, proton-exchange followed by heat treatment (Nakamura & Shimizu 1990), heat treatment with SiO_2 overlap (Fujimura *et al* 1991), and lithium out-diffusion (Webjorn *et al* 1989) near the Curie temperature (1000 ~ 1100°C) on the $+Z$ surface of $LiNbO_3$ plates.

The conversion efficiency of quasi-phase matching second harmonic generation in channel waveguide geometry can be expressed as follows (Jaskorzynska *et al* 1990):

$$\eta = \frac{8\pi^2 d_{33}^2 P^{\omega}}{c\varepsilon_0(\lambda^{\omega})N^{\omega}(N^{2\omega})^2 A_{\text{eff}}} \left| \int_0^L \exp(i\Delta k(z))z \, \mathrm{d}z \right|^2, \quad (2)$$

where λ^{ω} and P^{ω} are the fundamental wavelength and power in the waveguide, d_{33} is the SHG coefficient of $LiNbO_3$, and N^{ω} and $N^{2\omega}$ are the mode indices at the fundamental and harmonic wavelengths. The integral squared term within brackets describes the effect of the phase mismatch, where, in the perfectly uniform QPM waveguide, $\Delta k = N^{2\omega} - N^{\omega} - 2\pi q/\Lambda_0 = 0$, q being the grating order and Λ_0 the fundamental grating period. A_{eff} is the effective interaction area which describes the mode field overlap between the fundamental and the second harmonic modes as well as the profile of the domain inversion, and is given by (Jaskorzynska *et al* 1990):

$$A_{\text{eff}} = q^2 \bigg/ \left[\int_{-\infty}^{0} K(x,y)\varepsilon_m^{2\omega}(x,y)\varepsilon_n^{\omega}(x,y)\varepsilon_n^{\omega}(x,y)\mathrm{d}x\,\mathrm{d}y \right], \quad (3)$$

where ε_i represents the modal field of the ith mode at the superscript frequency and $K(x, y)$ depends on the grating profile. Two of the most critical factors in the conversion efficiency are the phase-matching factor [described by the term in the bracket of (2)] and the effective interaction area. The issue of phase matching as related to the waveguide nonuniformity has been reported recently (Cao *et al* 1991a). In this paper, we will address issues related to the problem of optimization of the effective interaction area.

In $LiNbO_3$, the domain inverted region, obtained by titanium indiffusion near the Curie temperature, is quasi-triangular in shape, as shown in figure 1. By controlling the titanium thickness and the diffusion conditions (temperature and time), different grating depths, h, can be obtained. However, in the case of periodic domain inversion, the grating depth is limited to the value when adjacent triangles start to overlap with one another. In our approach, in order to optimize conversion efficiency, first priority is given to the condition of non-critical phase matching waveguide dimension, next we address the condition of sufficiently recovered nonlinear coefficient. In addition, it is essential that the waveguide remains single moded at the fundamental wavelength in order to achieve improved beam confinement and reduced propagation loss. Finally, given the specific optimized waveguide dimensions, an appropriate grating depth can be chosen to minimize the effective interaction area. We will illustrate our optimization procedure using the following example. First, the waveguides have to be sufficiently annealed to restore the d_{33} coefficient (Cao *et al* 1991c). For better than 80% restoration of the nonlinearity (Cao *et al* 1991c), the surface index change $\Delta n^{\omega} \leqslant 0{\cdot}01$ and the index

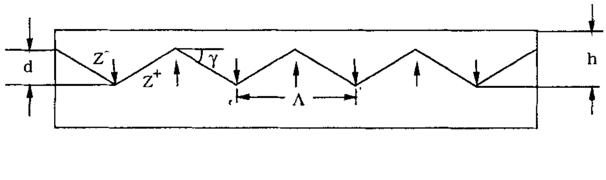

Figure 1. Triangular profile of the periodic domain inversion grating induced by titanium in-diffusion in $LiNbO_3$. h is the depth of the triangular grating.

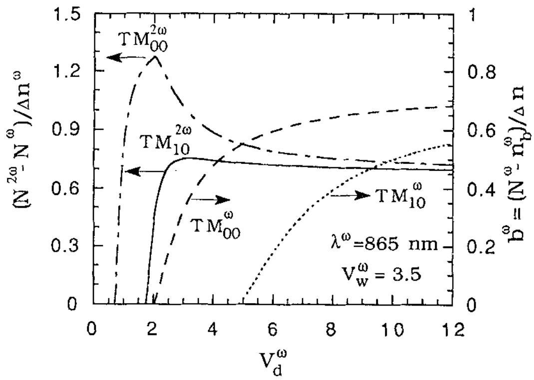

Figure 2. Normalized mode index mismatch between the fundamental ($TM_{00}^{2\omega}$) and the harmonic ($TM_{00}^{2\omega}$ and $TM_{10}^{2\omega}$) modes and normalized mode indices for TM_{00}^{ω} and TM_{10}^{ω} modes in APE $LiNbO_3$ channel waveguides as a function of normalized waveguide depth V_d^{ω} ($\lambda^{\omega} = 865$ nm).

profile can be approximated to a Gaussian profile (Cao *et al* 1991b). Next, we determine the mode index mismatch between the fundamental and the second harmonic as a function of the normalized channel waveguide depth $V_d^{\omega} = (2\pi/\lambda^{\omega})d_x(2n_b^{\omega}\Delta n^{\omega})^{\frac{1}{2}}$. Here n_b^{ω} is the substrate index and d_x is the depth of the index profile of the annealed waveguide. In figure 2, we present the normalized mode index mismatch between the fundamental (TM_{00}^{ω}) mode at fundamental wavelength and the fundamental and first-order ($TM_{00}^{2\omega}$ and $TM_{10}^{2\omega}$) modes at harmonic wavelength. The normalized mode indices of the TM_{00}^{ω} and TM_{10}^{ω} modes at the fundamental wavelength are also shown in order to indicate the range for single mode operation ($2 < V_d^{\omega} < 5$). We have chosen the waveguide depth $d_x = 3{\cdot}3\,\mu$m and $\Delta n^{\omega} = 0{\cdot}01$ to yield $V_d^{\omega} = 5$, at which the phase-matching condition is less sensitive to the depth fluctuations and the waveguide is still single-moded at the fundamental wavelength. As previously discussed, the choice of the channel width is not very critical, we have chosen the channel width to be around $6 \sim 7\,\mu$m in order to obtain better input coupling. After selecting the optimal waveguide geometry, we have calculated the inverse of the effective area A_{eff} as a function of the grating depth for $q = 1$, 2, 3 in APE channel waveguides using the theory outlined elsewhere (Cao *et al* 1991c). The results of the calculation are shown in figure 3, the maximum grating depth which can be implemented by titanium in-diffusion is also shown for the three grating orders. It is seen that the conversion efficiency strongly depends on the grating depth. By comparing the conversion efficiency for the various grating orders with respect to the grating depths which can be implemented, the second order QPM scheme appears to be the optimal structure. In addition, we also noticed that only in the case of first-order grating, the conversion efficiencies for the $TM_{00}^{2\omega}$ and $TM_{10}^{2\omega}$ modes are comparable. For the $q = 2$ and $q = 3$ cases, highest efficiency is achieved when the second harmonic generation occurs at the higher-order modes. These calculations also indicate the importance of using a first-order grating since an improvement by a factor of five over the $q = 2$ case and of ~ 10 over the $q = 3$ case, may be obtained in to the desired $TM_{00}^{2\omega}$ mode. Although the achievable grating depth of the first-order grating in $LiNbO_3$ is limited by the lateral overlap of titanium diffusion-induced triangular domain inversion, the situation is expected to be greatly improved in the case of $LiTaO_3$.

To confirm our theoretical predictions, we fabricated several periodic domain-inverted second-order QPM ($q = 2$) gratings ($\Lambda_0 = 6{\cdot}8\,\mu$m) with different grating depths on the $LiNbO_3$ Z^+ surface by titanium in-diffusion. $5 \sim 10$ nm thick titanium stripes were diffused for $1 \sim 1{\cdot}5$ h at $1075 \sim 1100$°C. The grating depth is easily revealed by barely etching the Y^+ surface. Two different grating depths (1·7 and 2·0 μm) were obtained using different diffusion conditions. A set of 5 mm long channel waveguides

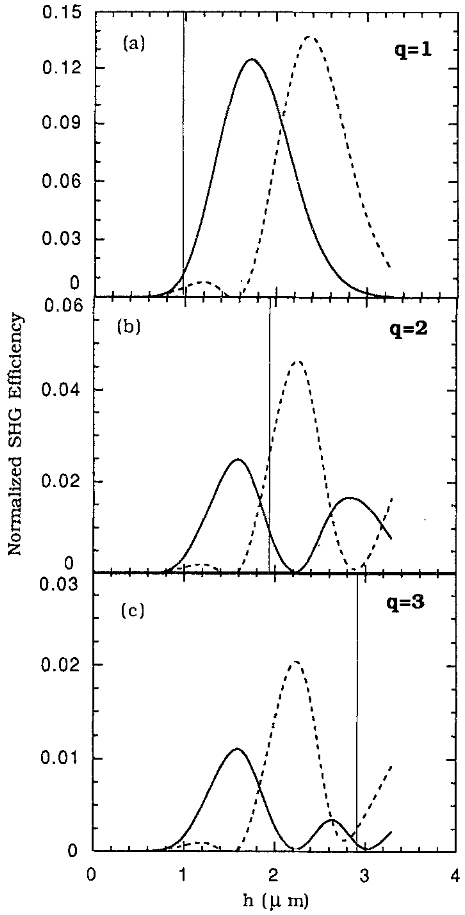

Figure 3. The SHG conversion efficiency (normalized to ideal laminar structure) as a function of domain inversion grating depth h for $TM_{00}^{2\omega}$ (————) and $TM_{10}^{2\omega}$ (-----) modes in the case of (**a**) first-, (**b**) second-, and (**c**) third-order QPM SHG in the optimized APE $LiNbO_3$ channel waveguides ($\lambda^{\omega} = 865$ nm).

with different channel widths ($2 \sim 10\,\mu$m) were fabricated by proton exchange from pure benzoic acid at 200°C for 0·7 h. The exchange was performed in a closed glass container, immersed in an oil bath which was stirred in order to achieve temperature uniformity of 0·25°C/cm. The waveguides were annealed for 10 h at 350°C in a furnace. Nearfield measurement of the mode field distribution indicates that the annealed guides have nearly Gaussian index profiles in both directions and waveguide depths are close to the optimum value of 3·3 μm. For channel guides with widths larger than 3 μm, the propagation loss at the fundamental wavelength is less than 0·5 dB/cm.

The frequency doubling experiment was performed using a tunable Ti-sapphire laser (Schwartz Electro-Optics). The output was spatially filtered and launched into the waveguide by end-fire coupling. The desired TM polarization was achieved by a Babinet–Soleil compensator. The second harmonic mode profile was monitored with a CCD camera. At 200 mW of laser output power, a typical value of 50 mW IR waveguide output power can be obtained. The phase matching bandwidth in the pump wavelength was measured using a wavemeter. The experimental results, summarized in table 1, indicate that one can obtain optimum conversion efficiency in a given SHG guided mode by choosing the appropriate grating depth as predicted by our theoretical calculation.

The temporal stability of the SHG output was also studied. At 50 mW IR power in the waveguide, the blue SHG output was found to be stable within an 8% fluctuation over a ten-hour period, and no sign of photorefractive damage was observed for either the

Table 1. Results of second harmonic generation experiment.

Sample	#1	#2
Grating depth	$1{\cdot}7\,\mu m$	$2{\cdot}0\,\mu m$
Waveguide output power ($\lambda^{\omega} \sim 865$ nm)	58 mW	52 mW
SHG power	$167\,\mu W$ ($TM_{00}^{2\omega}$) $32\,\mu W$ ($TM_{10}^{2\omega}$)	$43\,\mu W$ ($TM_{00}^{2\omega}$) $257\,\mu W$ ($TM_{10}^{2\omega}$)
Phase matching bandwidth	$0{\cdot}2$ nm ($TM_{00}^{2\omega}$) $0{\cdot}16$ nm ($TM_{10}^{2\omega}$)	$0{\cdot}2$ nm ($TM_{00}^{2\omega}$) $0{\cdot}17$ nm ($TM_{10}^{2\omega}$)
Phase matching length	$3{\cdot}25$ mm ($TM_{00}^{2\omega}$) $3{\cdot}94$ mm ($TM_{10}^{2\omega}$)	$3{\cdot}25$ nm ($TM_{00}^{2\omega}$) $3{\cdot}82$ mm ($TM_{10}^{2\omega}$)
Normalized conversion efficiency	47%/W-cm^2 ($TM_{00}^{2\omega}$) 6%/W-cm^2 ($TM_{10}^{2\omega}$)	10%/W-cm^2 ($TM_{00}^{2\omega}$) 65%/W-cm^2 ($TM_{10}^{2\omega}$)

fundamental or harmonic light. We also noticed that the effective phase matching length for the $TM_{10}^{2\omega}$ mode is longer than that for the $TM_{00}^{2\omega}$ mode. This result is also consistent with the theoretical calculation shown in figure 2, since the mismatching between the propagation constant of the fundamental and the harmonic ($TM_{10}^{2\omega}$) modes is less sensitive to the variations in the waveguide depth. The higher conversion efficiency for the $TM_{10}^{2\omega}$ mode is thought to be primarily due to the grating depth and the long effective phase matching length. In addition, as illustrated in figure 3, further improvement in the conversion efficiency is expected when the proper grating depth of $2{\cdot}2\,\mu m$ is obtained.

3. Conclusions

In conclusion, we have analysed SHG conversion efficiency for the first, second and third-order QPM gratings by taking into account the effect of the triangular shape of the domain inversion implemented by titanium diffusion. From the dependence of the grating depth on the conversion efficiency and the depth limitation of triangular domain inversion, we have shown that the second-order QPM grating is superior to the first- and third-order gratings. This prediction is further confirmed by our experimental results where, by using a second-order QPM grating, harmonic blue light of 0·26 mW at 432 nm wavelength was generated in a five-millimetre annealed proton-exchanged $LiNbO_3$ waveguide for a normalized conversion efficiency of 65%/W-cm^2. Although this conversion efficiency is still about a factor of 2 lower than the theoretical limit, the efficient blue harmonic generation demonstrated here constitutes a major improvement over previously published results and illustrates the importance of utilizing second-order QPM gratings.

References

Bloembergen N, Sievers A J 1970 Nonlinear optical properties of periodic laminar structures. *Appl. Phys. Lett.* 17: 483–485

Cao X F, Natour J, Ramaswamy R V, Srivastava R 1991a Effect of waveguide uniformity on phase matching for frequency conversion in channel waveguides. *Appl. Phys. Lett.* 58: 2331–2333

Cao X F, Natour J, Ramaswamy R V, Srivastava R 1991b *Tech. Dig. Gradient Index Optical System GRIN' 91* (Washington DC: Opt. Soc. Am.) Paper Tu 3

Cao X F, Srivastava R, Ramaswamy R V, Natour J 1991c Recovery of 2nd order optical nonlinearity in annealed proton exchanged $LiNbO_3$. *IEEE J. Photonics Technol. Lett.* 3: 25–27

Fejer M M, Lim E J 1990 *Tech. Dig. Integrated Photonics Research, IPR'90* (Washington, DC: Opt. Soc. Am.) paper Tu 11

Fujimura M, Suhara T, Nishihara H 1991 Ferroelectric-domain inversion induced by SiO_2 cladding for $LiNbO_3$ waveguide. *Electron. Lett.* 27: 1207–1209

Jaskorzynska B, Arvidsson G, Laurell F 1986 *SPIE* 651: 221–228

Laurell F, Webjorn J, Arvidsson G 1990 *Tech. Dig. Integrated Photonics Research, IPR'90* (Washington, DC: Opt. Soc. Am.) Paper Tu 12

Lim E J, Fejer M M, Byer R L 1989 Second harmonic generation of green light in periodically poled planar lithium niobate waveguide. *Electron. Lett.* 25: 174–175

Nakamura K, Shimizu H 1990 Ferroelectric inversion layers formed by heat treatment of proton exchanged $LiTaO_3$. *Appl. Phys. Lett.* 56: 1535–1537

Webjorn J, Laurell F, Arvidsson G 1989 Blue light generated by frequency doubling of laser diode light in lithium niobate waveguide, *IEEE Photonics Technol. Lett.* 1: 316–318